European Polymer Journal 84 (2016) 54–64

Contents lists available at ScienceDirect

European Polymer Journal

journal homepage: www.elsevier.com/locate/europolj

Double stimuli-responsive polymer systems: How to use crosstalk between pH- and thermosensitivity for drug depots

A. Bogomolova [a], L. Kaberov [a], O. Sedlacek [a], S.K. Filippov [a], P. Stepanek [a], V. Král [b], X.Y. Wang [c], S.L. Liu [c], X.D. Ye [c], M. Hruby [a,*]

[a] Institute of Macromolecular Chemistry AS CR, v.v.i., Heyrovsky Sq. 2, 162 06 Prague 6, Czech Republic
[b] University of Chemistry and Technology Prague, Technicka 5, 166 28 Prague 6, Czech Republic
[c] Department of Chemical Physics, Hefei National Laboratory for Physical Sciences at the Microscale, University of Science and Technology of China, Hefei, Anhui 230026, PR China

ARTICLE INFO

Article history:
Received 15 July 2016
Received in revised form 6 September 2016
Accepted 8 September 2016
Available online 12 September 2016

Keywords:
Drug depot formulation
Double responsive system
pH-responsive polymer
Thermoresponsive polymer

ABSTRACT

We describe a new approach to depot drug delivery in which a copolymer poly[*N*-isopropyl acrylamide-*co*-*N*-(3-imidazolylpropyl)methacrylamide] (PNIPAM-*co*-ImPM) is considered as the main object and matrix for a new formulation strategy that provides the controlled and sustained release of an incorporated drug. The relatively low content of ImPM groups (1.6 mol%) was determined to be sufficient to introduce pH-sensitive behavior to the polymer. Together with NIPAM units, which possess a thermo-sensitive behavior, a dual sensitivity was imparted to the polymer that was investigated by means of turbidimetry and dynamic light scattering. A change in pH from 9 down to 4 was observed to result in the increase of the polymer transition temperature from 32 to 70 °C. The separation process is also accompanied with the formation of ca. 150–300 nm particles while above the transition temperature. The pH value of approximately 6.5 was defined as a boundary value, where certain properties of the system significantly change. This observation assumes a potential attractiveness of the system for biological applications in which injection is possible using a liquid form at pH ca. 5 without the risk of injection needle obstruction. In this way, a depot is formed at the application site upon simultaneously heating to body temperature and increasing the pH to the physiological value of 7.4. An in vivo experiment using the polymer in PBS (pH = 5.0) with paliperidone as a model drug showed excellent results regarding the release of the drug from a depot. The putative mechanism of action for our depot system is thoroughly described in the article.

1. Introduction

Depot formulations have attracted considerable interest in contemporary pharmaceutical research because they allow for maintaining a steady blood concentration of the active pharmaceutical ingredient (API) for up to several weeks after injection. This is especially advantageous for antipsychotics in which the suppression of the fluctuation of serum levels leads to a decrease in dosage and side effects while keeping or even improving treatment efficacy [1–6]. Last but not least, such formulations are advantageous for non-cooperating patients that may not follow a physician's instructions. The typical depot

* Corresponding author.
E-mail address: mhruby@centrum.cz (M. Hruby).

http://dx.doi.org/10.1016/j.eurpolymj.2016.09.010
0014-3057/

formulation contains the drug encapsulated in polymer or another matrix, which after injection forms a local depot that gradually dissolves and releases the API [1–6]. Many depot formulations require organic solvents or oil as vehicular, and such injections often cause local inflammations and pain as a common side effect [7], with oil embolisms also being a common complication [8]. Alternatively, poorly water-soluble microcrystalline prodrugs are applied intramuscularly where they are gradually enzymatically cleaved, e.g., by esterases, into active drugs that are then released from the depot [9–11]. A disadvantage of this type of system is the fluctuation of local concentrations of activating enzymes within a single patient and also among different patients.

The use of micro- and nanoparticles in combination with polymers (e.g., poly(lactide-*co*-glycolide) [12–15] is another type of depot formulation. Here, it is possible to reach a sustained release in a diffusion-controlled or matrix degradation-controlled manner, however, with similar problems considering that the predictability of sustained release is due to the aggregation and hard-to-set diffusion rate of the drug within the polymer matrix [5,15–19].

Thermoresponsive polymers possessing a lower critical solution temperature (LCST) in the range between room and body temperatures allow the administration of the formulation as a liquid in an aqueous milieu; while after the phase separation induced by the body temperature, the depot is formed [20–25]. The phase-separated thermoresponsive polymer, after phase separation, regulates the release of the drug in a diffusion barrier-like manner from such a depot [7–12,20,22,23,25]. However, the main issue may be the obstruction of the needle during injection because phase separation is fast and the well heat-conducting metallic needle reaches surrounding (body) temperature quickly [26–29]. The solution to this problem may be the application of an organic solvent, such as dimethyl sulfoxide (where the polymer is soluble but without a LCST), or as newly described in this paper, to use a polymer with dual responsivity that makes its application in aqueous milieu possible.

For imidazole-containing polymers, the pH-responsivity of imidazole (pK_a ca. 7 depending on the functionalization) allows one to inject the system in a mildly acidic yet biologically acceptable milieu (pH 4.5–5.5), where imidazole is protonated and highly hydrophilic. The charged state of the imidazole units shifts the transition temperature of the polymer solution to higher values [30]. With a pH increase to 7.4 in tissue, imidazole is mostly deprotonated, resulting in a phase separation of the system at temperatures significantly lower than in the former case. Thus, the phase separation temperature drops, and it becomes possible to create a system that is injectable without needle stroke under one set of conditions (low pH value, cloud point temperature - CPT above body temperature), while it forms a depot or nanostructured scaffold in tissue under another set (higher pH value, CPT below body temperature). While the approach of dual temperature and pH responsiveness has already been well described in a number of publications [31–34], here, in this paper, we report on the synthesis and solution properties of copolymers of *N*-isopropyl acrylamide (NIPAM) and *N*-(3-imidazolylpropyl)methacrylamide (ImPM) that are specifically intended for parenteral depot drug delivery applications. Here, the NIPAM monomeric units introduce a thermosensitivity to the copolymer, while the ImPM monomeric units bring pH-responsiveness. A number of copolymers with different ratios of monomers were synthesized by RAFT polymerization. The polymer composition (molar ratio of NIPAM and ImPM units) has a crucial influence on the solution properties of copolymers, primarily on the value of the transition temperature. It was proven by dynamic light scattering that the copolymers possess a reversible association behavior with changing pH and temperature. The conditions of pH range 5–8 and temperatures of 35–39 °C are considered to be ideal for the intended use. The model antipsychotic drug paliperidone (as palmitic acid salt) was incorporated into the system, and a polymer-controlled sustained release was demonstrated in an in vivo model and compared with the release profile for the prodrug paliperidone palmitate (ester). Therefore, the same drug release profile is feasible with just the salt of the active drug instead of the necessity of the enzymatically activated prodrug (with all its drawbacks related to fluctuating local enzymatic activity levels), which also brings significant simplification of further approval procedure.

2. Materials and methods

2.1. Materials

N-Isopropylacrylamide, 1-(3-aminopropyl)imidazole, 2-cyano-2-propyl benzodithioate, methacryloyl chloride, and 2,2′-azobis(2-methylpropionitrile) (AIBN) were purchased from Sigma-Aldrich Ltd. (Czech Republic). Dichloromethane, 1,4-dioxane (99.8%), methanol, diethyl ether, NaOH, NaCl, Na_2SO_4 were purchased from Lach-Ner (Czech Republic). *N*-Isopropylacrylamide was recrystallized from hexane. *o*-Nitrobenzaldehyde (*o*-NBA) was recrystallized twice from ethanol before use. AIBN was recrystallized from acetone. All other chemicals were used without additional purification. Sephadex G-25 was obtained from Amersham Biosciences (Sweden). Paliperidone palmitic acid salt was provided by Zentiva, Sanofi generics.

2.2. Synthesis of N-(3-imidazolylpropyl)methacrylamide (ImPM, see Fig. 1)

The 1-(3-aminopropyl)imidazole (7.50 g, 60 mmol) was dissolved in dichloromethane (7.15 mL). With cooling by an ice bath and vigorous stirring, an aqueous solution of sodium hydroxide (2.56 g, 64 mmol) (20 mL) and then subsequently methacryloyl chloride (6.96 g. 60 mmol) in dichloromethane (6.5 mL) were added dropwise. The mixture was allowed to heat to room temperature, and then the organic layer was separated. The water phase was extracted twice with dichloromethane, and the combined organic layers were washed with saturated sodium chloride solution. The organic solution

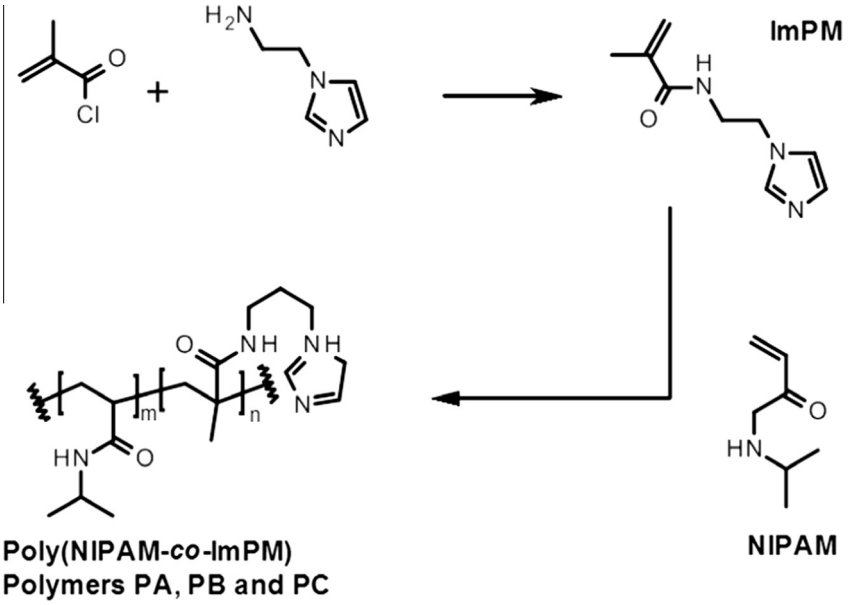

Fig. 1. Synthetic route for preparing poly(NIPAM-*stat*-ImPM) copolymers.

was then dried over magnesium sulfate and concentrated to ca. 10 mL *in vacuo*. The crude product was purified by flash-chromatography on spherical silica using methanol-chloroform (15:85 v/v) as the eluent. Finally, the monomer was isolated as a colorless oil product.

N-(3-Imidazolylpropyl)methacrylamide ($C_{10}H_{15}N_3O$): Yield 1.2 g (16%) of colorless oil. ^{1}H NMR ($CDCl_3$): δ = 1.92 (s, 3H), 2.02 (q, 2H), 3.3 (q, 2H), 4.0 (t, 2H), 5.3 (s, 1H), 5.68 (s, 1H), 6.7 (s, 1H), 6.95 (s, 1H), 7.02 (s, 1H), 7.63 (s, 1H), ^{13}C NMR (151 MHz, $CDCl_3$) δ 169.01 (C═O), 139.81 (CH_2═$CH(CH_3)$—), 137.17 (—N—CH═CH—N═CH—), 128.80 (—N—CH═CH—N═CH—), 119.94 (CH_2═$CH(CH_3)$—), 119.15 (—N—CH═CH—N═CH—), 45.00 (—N—CH_2—CH_2—CH_2), 36.89 (—N—CH_2—CH_2—CH_2), 31.10 (—N—CH_2—CH_2—CH_2), 18.79 (CH_2═$CH(CH_3)$—), MS-ESI: 216.08 $[M+Na]^+$ (100%), 194.17 $[M+H]^+$ (9.5%). The ImPM monomer easily undergoes spontaneous polymerization during storage, even at low temperature, so it should be worked up for polymerization as fast as possible.

2.3. Synthesis of polymers (see Fig. 1)

The reversible addition–fragmentation chain transfer (RAFT) polymerization was performed with 2-cyano-2-propyl benzodithioate as a chain transfer agent. A mixture of the monomers *N*-(3-imidazolylpropyl)methacrylamide (ImPM, 0.85 mmol for polymer PA, 1.26 mmol for polymer PB, and 1.6 mmol for polymer PC) and *N*-isopropylacrylamide (NIPAM) (to a total monomer amount of 16 mmol), the chain transfer agent (0.15 mmol) and AIBN (0.03 mmol) were dissolved in 1,4-dioxane (7 mL). The polymerization mixture was flushed with argon for 10–15 min followed by polymerization at 75 °C for 16 h. The reaction mixture was cooled to room temperature, and the crude polymer was precipitated in diethyl ether, filtrated and dried *in vacuo*. The yield was ca. 60% for all polymers. The resulting polymer was further purified by column chromatography with Sephadex LH-20 as a stationary phase and methanol as a mobile phase. After separation, the fractions containing the polymer were taken, the methanol was evaporated, and the residue was dissolved in THF, precipitated in diethyl ester and dried *in vacuo*.

The molecular weights of the polymers were determined by gel permeation chromatography (GPC) in a mixture of acetate buffer (pH 6.5; 0.3 mol L^{-1}) and methanol (20:80 v/v) as a mobile phase on a TSK 3000 SWXL column (Polymer Laboratories Ltd., UK) with an HPLC System Ultimate 3000 (Dionex, US) equipped with RI, UV and multiangle light-scattering DAWN DSP-F (Wyatt, U.S.A.) detectors. The weight-average molecular weights, M_w, for PA, PB, and PC were 11.2 kDa, 14.2 kDa and 26.3 kDa, respectively. The polydispersities, I ($I = M_w/M_n$, where M_n is the number-average molecular weight) were 1.39, 1.35 and 1.30 for polymers PA, PB and PC, respectively. The molecular characteristics of the synthesized copolymers are summarized in Table S1 (see Supporting materials).

The monomeric unit ratio of the copolymers was assayed by potentiometric titration because the determination of the monomer ratio by NMR analysis is not unequivocal in the current case (there is an overlap in the characteristic signals for NIPAM and ImPM groups (Fig. S1)). The copolymers contained 0.50, 2.0 and 3.7 imidazole moieties per polymer chain for polymers PA, PB and PC, respectively.

2.4. Experimental procedure of polymer characterization

All of the copolymer solutions used within the physico-chemical characterization of the system were prepared in deionized Milli-Q water. The concentrations of the polymers were chosen 4 mg/mL, if it is not stated differently. The adjustment of the solution pH value was performed by the addition of 0.2 M hydrochloric acid. The dual sensitivity of polymers to pH and temperature demands a certain methodology for the experiment. The experimental procedure chosen for the current system was the following. The determination of the phase-separation behavior was conducted in a stepwise manner: the change in pH was conducted first, then the temperature scan was performed, and then the polymer solution was recovered to the initial homogeneous state; thus, one step was completed and next step of the pH change was performed. Three physical parameters were measured for the polymer solutions, transmittance (with an UV–VIS spectrophotometer), light scattering intensity and hydrodynamic diameter.

2.4.1. Turbidity experiment

The cloud point temperature (CPT) was determined by measuring the change in the transmittance of the polymer solution as a function of the temperature. The transmittance was measured at $\lambda = 450$ nm, far away from the absorbance peak observed for *N*-(3-imidazolylpropyl)methacrylamide and its copolymers consequently, with an UV–VIS spectrophotometer (Thermo Scientific Evolution 220, equipped with a Thermo Scientific single cell Peltier element). Temperature was controlled manually, with average heating/cooling rate 1 °C/min and varied from 25 up to 70 °C. The cloud point temperature for the polymer solution at a particular pH was determined at 50% transmittance. A cooling experiment (hysteresis) was also conducted where necessary.

2.4.2. Dynamic light scattering experiment

The temperature dependencies of the apparent hydrodynamic diameter, D_h, and the light scattering intensity, I_s, of the copolymer solutions were determined at 173° using a Zetasizer Nano-ZS, model ZEN3600 (Malvern Instruments, U.K.). The DTS (Nano) program was used for data evaluation. It provides intensity-, volume-, and number-weighted D_h distribution functions, $G(D_h)$. The intensity-weighted value of the apparent D_h was chosen to monitor the temperature-dependent changes in the system.

Additionally, for transparent solutions below the CPT, dynamic light scattering experiments were carried out on an ALV instrument equipped with a 22 mW He–Ne laser. An ALV 6000, multibit, multi-tau autocorrelator covering approximately 12 decades of the delay time, τ, was used for the measurements of time autocorrelation functions. The obtained correlation functions were analyzed by REPCALC analytical software [35], providing a relaxation time distribution function, $W(\tau)$. The temperature was controlled within 0.05 °C. The prepared samples were filtered into dust-free cells. Experiments were conducted in an angular range: 40–150°. The diffusion coefficient, D, was obtained from the standard relation:

$$\Gamma = \tau^{-1} = D_{tr} q^2 \tag{1}$$

where Γ is the relaxation rate. The scattering vector is $q = 4\pi n \sin(\theta/2)/\lambda$, where λ is the laser wavelength, n is the refractive index of the solvent, and θ is the scattering angle.

Finally, the apparent intensity-weighted hydrodynamic diameter of particles, D_h, was calculated using the Stokes-Einstein equation.

If not otherwise stated, all measurements were conducted with 4 mg/mL polymer solutions, and all solutions were filtered through a 0.45 μm PVDF filter before measurement.

2.5. Kinetics of redissolution of phase-separated polymer upon a pH jump

A modified procedure according to Refs. [36,37] was used, briefly: A solution with a polymer concentration of 2 mg/mL and an *o*-nitrobenzaldehyde concentration of 10 mM was placed into a sample cell consisting of two quartz windows with a 200 nm spacer and thermostated at 35.0 °C. The pH jump was induced by irradiation with the third harmonic of an Nd:YAG laser at 355 nm. A 200 W high pressure mercury lamp with a long pass filter with a cutoff wavelength of 450 nm was used as a light-scattering source. A notch filter at 355 nm with a full width at half maximum (FWHM) of 17.8 nm was used to block the scattered 355 nm laser light. Scattered light from the phase-separated polymers was collected with a photomultiplier tube (Hamamatsu R928) and recorded on a Tektronix oscilloscope (TDS 3054B).

2.6. In vivo biological evaluation using paliperidone palmitate as a model drug

The formulation was prepared by the dissolution of copolymer PC (100 mg) in isotonic phosphate-buffered saline (PBS, pH 7.4, 0.5 mL). Microcrystalline paliperidone palmitic acid salt (crystal size 10–20 μm, 30 mg) was added, and the pH of the formulation was set to 5.0 with the addition of hydrochloric acid (1 mol/L). The originator of the formulation of paliperidone palmitic acid ester was Invega® Sustena® (Johnson & Johnson, NY, U.S.A.).

The determination of pharmacokinetics was performed on healthy female Wistar rats (animal weight 200–270 g at the beginning of the study), with 6 animals per group. The formulation was injected deeply i.m. a dose of 30 mg paliperidone

palmitate salt or paliperidone equivalent ester per animal. Blood samples were taken by a 10G needle at times 4 h, 8 h, 24 h, 3 days and 7 days after administration and then every week for 6 months. The blood was immediately transferred to a heparinized test tube and kept on ice until analysis. The samples were centrifuged at 2500 rpm at 5 °C for 15 min, and the plasma was transferred to polypropylene vials and stored at −70 °C until the time for analysis. The paliperidone content was determined by LC/MS/MS, as described elsewhere in Ref. [38]. All animal studies were performed in accordance with Czech Republic and European Union legislation and guidelines.

3. Results and discussion

Our first aim was to create polymers possessing dual pH and thermoresponsive behavior in the range of pH 5.5–7.4 and the temperature range 30–42 °C, respectively. The molecular weight was set to 20–25 kDa to allow for elimination by the kidneys after the redissolution of the depot [renal threshold is ca. 45 kDa for (meth)acrylamide-type polymers [39–42]]. Copolymers of *N*-isopropyl acrylamide with M_w below the renal threshold are partly eliminated to urine and partly to feces with no organ redeposition, as we demonstrated before [24]. The polymer/drug mixture is to be injected into a muscle at slightly acidic pH, approximately 5.0–5.5. Under this condition, the cloud point temperature of the polymer solution is higher than room and body temperatures, and the polymer only prevents the aggregation of hydrophobic drug crystals because of the association of the drug with the hydrophobic main-chain of the polymer. Thus, the polymer acts similarly to a local surfactant with a hydrophobic main-chain and polar pendant groups. The simultaneously increased temperature and pH in the muscle should result in the self-assembly of the polymer molecules because CPT is reduced, and a subsequent physical incorporation of the drug inside newly formed structures could be assumed (see Fig. 2). Simultaneously, the pH in the surrounding medium should be continuously changed from the acidic to neutral because of the pH and buffering capacity of bodily fluids. The buffering capacity of the copolymer solution should be kept as low as possible to accelerate this process; this is why the minimum amount of imidazole comonomer content was employed.

The RAFT polymerization was used for the synthesis of all of the polymers under investigation [43]. The implementation of this synthetic route is explained by a necessity to control the molecular weight of the polymers and to keep the molecular weight distribution as narrow as possible, which is essential for uniform biological behavior within each sample. The second reason comes from the dependency of the LCST value on the same molecular characteristics (molecular weight and molecular weight distribution) [44,45]. Two monomers were chosen for the synthetic route, *N*-isopropylacrylamide (NIPAM), copolymers of which possess a thermoresponsive behavior and are described to be negligibly cytotoxic [46–48], and *N*-(3-imidazolylpropyl)methacrylamide (ImPM), which is a pH-sensitive monomer. Other conditions for the synthetic

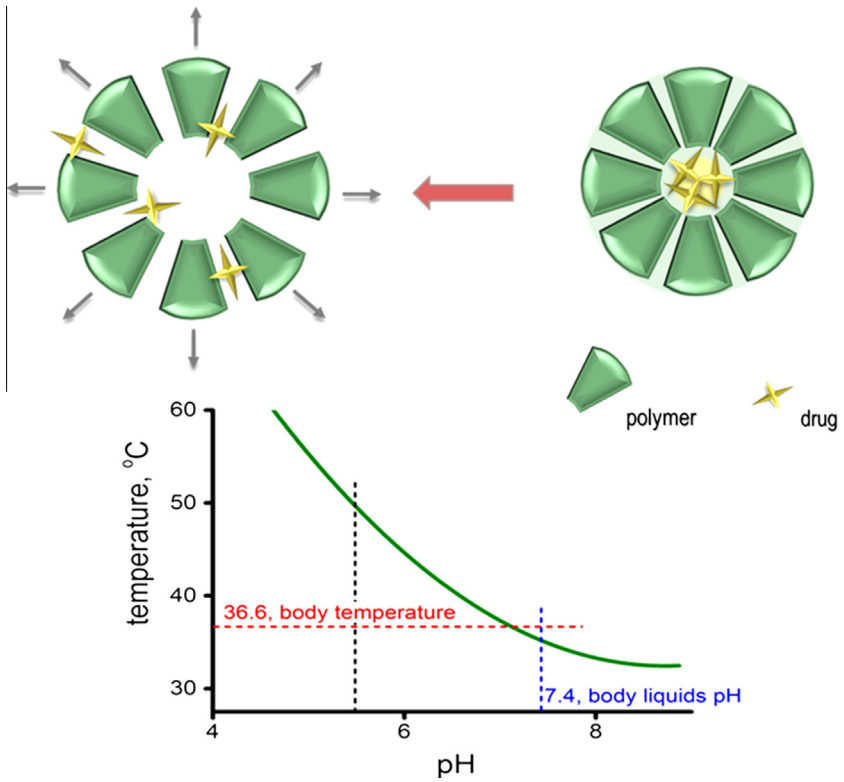

Fig. 2. Strategy for the depot drug delivery application described in this article.

procedure include using 2,2′-azobis(isobutyronitrile) (AIBN) as the initiator, 2-cyano-2-propyl benzodithioate as the chain transfer agent and 1,4-dioxane as the solvent. A variation in the content of pH-sensitive units was used for the regulation of solution behavior in the polymer solution. Consequently, a content of 1–2 mol% of ImPM units in the polymer is completely sufficient to fulfill the general requirements that have been applied to the polymer. Therefore, the polymers with a content of ImPM units in the range of 0.5 to 2.5 mol% were further used for the physico-chemical characterization. It is important that the ImPM units possess a weakly basic nature, and consequently, that they are hydrophilic at low pH and become hydrophobic with increasing pH values. This property is considered important to further understand the solution behavior of our statistical polymers.

The M_n value in all cases was in a range of 8.1 – 20.2 kDa with a dispersity of approximately 1.3–1.4 (see Fig. S2 in Supporting Materials for GPC chromatograms). Certain increase in M_w was observed with increase in the content of imidazole moieties. Due to ionic nature of imidazole groups, the formation of interchain associated may happened. That tendency should increase with increase in the number of imidazole groups and may explain the result of GPC measurement [49]. To comment possible distribution of imidazole unit along polymer chain, the transfer behavior of the monomers has to be considered. We used a methacrylamide-type imidazole monomer to be copolymerized with *N*-isopropyl acrylamide because of isolation and handling problems connected with the use of the corresponding acrylamide analog (namely, with its tendency to undergo spontaneous uncontrolled polymerization). This was performed in analogy to the common use of *N*-isopropyl methacrylamide to fine-tune the CPT of *N*-isopropyl acrylamide [50,51]. In addition, the pH-dependent phase separation behavior (see below) shows that the polymer with the highest imidazole monomer content, which was used for most of the studies, is sufficiently molecularly homogeneous. This is because the onset of the phase separation – the CPT - depends strongly on pH, and the phase separation is sharp in a very narrow temperature range for all pH (see Fig. 3, which would not be the case if there was a significant amount of polymer chains with different monomer compositions). Furthermore, the low amount of imidazole moieties compared to the theoretical value allow to suppose the low reactivity of ImPM compared to NIPAM monomer. Thus, the statistical or gradient structure seems to be a most plausible assumption for current polymers. Further rigorous detailed determination of the monomer reactivity ratios is beyond the scope of an applied polymer paper, such as this one. Potentiometric titration used for the composition calculation was also exploited to provide data about the pK_a value. pK_a = 4.6 was found for polymer PC with the highest content of ImPM groups, and it increases up to 5.4 (0.5 mol% ImPM for polymer PA) with decreasing numbers of pH-sensitive units. This is in agreement with the theory that protonation of the first imidazole moieties on the polymer chain shifts the pK_a of the other imidazole moieties on the same polymer chain down in the pH scale because of columbic repulsion between the incoming protons and the already positively charged polymer chain [52].

Polymer PC was chosen for a more detailed investigation regarding the physico-chemical properties of the polymer solution because of it having the highest homogeneity of monomeric composition of the copolymers with respect to the nature of copolymerization and the number of imidazole comonomer moieties per chain. The turbidity experiment was conducted first to determine the phase-separation behavior for a wide range of pH values. The experiment was performed in a stepwise manner, as described in the Materials and method section. The cloud point temperature for the polymer solution at a particular pH was determined at 50% transmittance. The results from the turbidity experiment are presented in Fig. 3.

It is visible from the turbidity curves that the cloud point temperature continuously shifted to higher values while the pH of the system decreased. This shift is more prominent in range of pH values from 5.7 to 4.5, which is in close vicinity to the pK_a value of our polymers. In this particular range, a transition takes place from a slightly charged state to a completely charged state of the polymer. These charges on the polymer chain, even at a considerably low concentration, effectively postpone the separation process. Furthermore, when the pH drops below the pK_a value, the free H^+ in the hydration layer

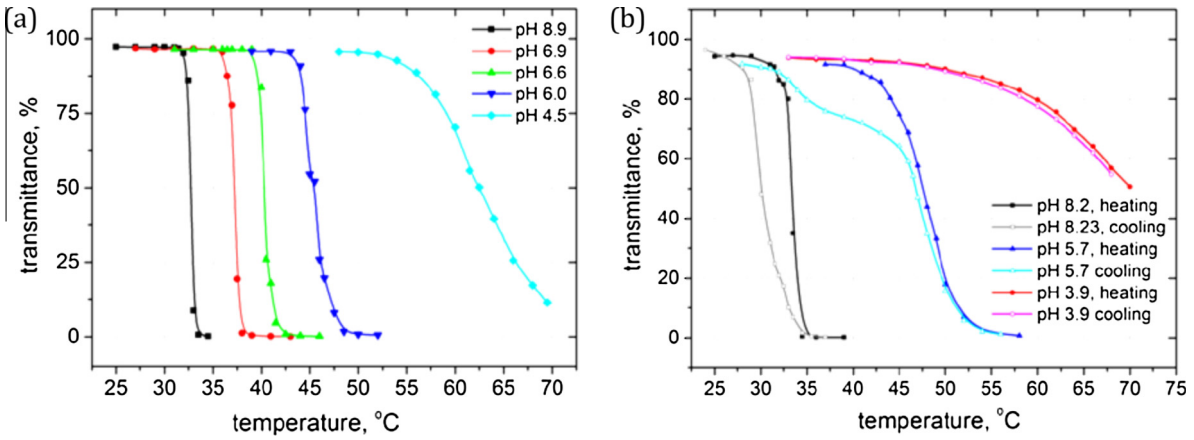

Fig. 3. Temperature induced turbidity changes evaluated through the reduction in the transmittance of the PC polymer solution, c = 4 mg/ml (a) during the heating process and (b) during the heating and cooling processes.

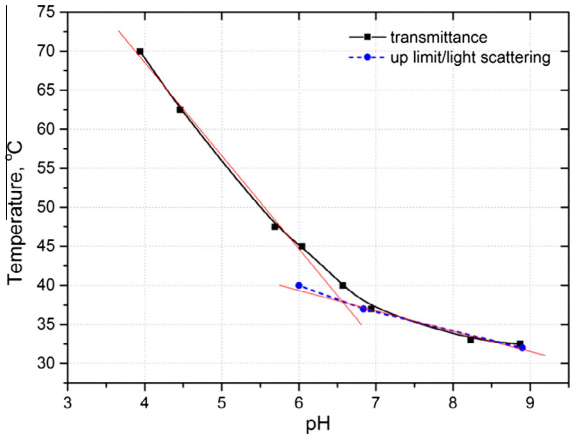

Fig. 4. Diagram of the shift in the cloud point temperature of the PC polymer solution (c = 4 mg/ml) depending on the solution pH.

of the polymer appear to stabilize the polymer chains and prevent a complete separation process. As a summary of this explanation, the diagram in Fig. 4 is presented. It becomes clear from Fig. 4 that the T(pH) dependency is characterized by a nonlinear trend. The same conclusion has been made by Maeda et al., who determined that such behavior for poly (*N*-isopropyl-acrylamide-*co*-*N*-vinylimidazole), poly(*N*,*N*-diethylacrylamide-*co*-*N*-vinylimidazole) and poly(*N*-vinylcaprolactam-*co*-*N*-vinylimidazole) copolymers yielded a sigmoidal curve [53,54]. The reason for such behavior could be found in the number of forces and interactions that contribute to the association process, namely, the hydrophobic interactions between isopropyl pendant groups, hydrogen bonds between the amine proton and carboxylic oxygen in the NIPAM units and the electrostatic repulsion between charged imidazole-containing units. Thus, a gain or reduction in certain forces would define the general behavior of the whole system and, as a consequence, the nonlinear character of the T(pH) curve. By attempt to figure out the pH value, where significant change in character of T(pH) curve takes place, we made an extrapolation of linear parts of T(pH) curve. Since at acidic pH's the ionization of ImPM units should proceeds, we attribute the cross point of linear fits with a point, when the electrostatic interaction start to play a crucial role in interchain association.

The transition temperature data obtained from dynamic light scattering intensity are presented in Fig. 4. One can note that the transition temperature acquired from the DLS measurements are lower than those values determined from the turbidity experiment. Such discrepancy is a general manifestation of the different sensitivities of the two methods. The DLS measurements were performed over a broad temperature range below and above the CPT [55]. The results of these experiments are presented in Fig. 5 and Figs. S2–S11 in Supporting materials.

Several things can be noted from Fig. 5. In agreement with the turbidity data, the diameter of the particles manifests the existence of a threshold temperature above which the nanoparticle size grows approximately two orders of magnitude. The threshold position (CPT) and the aggregate size are pH sensitive values. Below the CPT a distribution function over the relaxation times shows a bimodal distribution with a dominant fast mode (Figs. S2 and S3, S7–S10 in Supporting Materials).

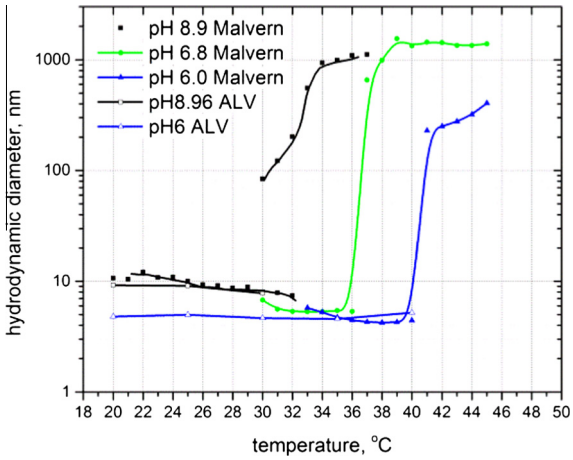

Fig. 5. DLS data from polymer PC, where c = 4 mg/mL. Solid points were obtained from a Zetasizer Nano-ZS at $\theta = 173°$; open points were obtained from an ALV set-up by extrapolation to a zero scattering angle, according to the procedure described in the Materials and methods.

The apparent hydrodynamic diameter obtained by the extrapolation of relaxation times to a zero scattering angle has a value of 6–10 nm and can be attributed to molecularly dissolved polymers. D_h values obtained from the single angle experiment (Zetasizer Nano-ZS) and from the extrapolation to a zero scattering angle (ALV) have good agreement (Fig. 5). The slow mode was attributed to a small fraction of aggregates that are present in the solution. Upon heating above the CPT, the distribution functions over the relaxation times show the presence of a dominant slow mode (Figs. S4 and S11 Supporting Materials). Because of significant multiple scattering, DLS experiments above the CPT were conducted with the Zetasizer Nano-ZS set-up. The aggregate size above the CPT at a pH value of 8.9 more than two times exceeds the size of the same particles at a pH value of 6.0. One can assume that because of strong repulsive electrostatic forces below pH 6.5, the polymer chains start to phase separate at higher temperatures. Simultaneously, full-grown aggregates have smaller sizes at low pH values because of the stabilization effect of the electrostatic forces between charges on the polymer chains. At this point in experimentation, the role of hydrogen bonds in the association process was left undefined. To make it more clear, the heating and cooling turbidity experiments were performed (see Fig. 3b). As is revealed, a hysteresis effect was observed for the cases of high pH and pH values above pK_a. The hysteresis is an effect that is typical for PNIPAM solutions, and it is usually attributed to the formation of inter- and intra-molecule hydrogen bonds [55,56]. Thus, hydrogen bonds are preserved in the system even when the polymer is partly charged (pH = 5.7). This effect may play a significant role in our depot drug delivery strategy.

The important aspect of our strategy is the rate of pH-change-driven phase separation, which should be as fast as possible in this case to assure immediate depot formation without an immediate washing-out effect. Another point is the rate of the redissolution process that is responsible for polymer elimination from the organism after fulfilling its task (as we have previously shown with a radiolabeled polymer, the polymer depot gradually dissolves due to the continuous washing of the depot with bodily fluids and the re-equilibration between the phase-separated and dissolved fractions of the polymer) [24]. While the phase separation of *N*-isopropylacrylamide copolymers involved in this study is very fast (too fast to be measured by a benchtop UV–VIS spectrophotometer, data not shown), the redissolution may be substantially slower depending on the rearrangement of hydrogen bonds and the entanglements of polymer chains.

It is unlikely that the use of a photobase is problematic because of the limited availability of suitable photobases that are sufficiently hydrophilic to be water-soluble in this case, therefore, we can study the kinetics of redissolution upon acidification using a photoacid after pulse laser irradiation. For example, the pH-jump can be induced by a proton release from *o*-nitrobenzaldehyde after irradiation with a 355 nm pulse laser [13,14,57,58]. Redissolution may then be followed by recording the scattered light intensity after irradiation. We have performed this experiment to have better insight into crosstalk between pH and thermoresponsivity mainly as curiosity driven research, but these data are also relevant from the practical point of view – temporary acidification in the depot site may occur if there will develop inflammation in the tissue or after high physical exercise of the muscle, where acidification occurs due to partial switching to anaerobic lactic acid metabolism. This may eventually lead to accelerated depot redissolution. As a preliminary study, Fig. 6 shows that a 1 s irradiation by a continuous UV source (Hamamatsu, LC8) was sufficient to completely dissolve the polymer. The redissolution process is very fast, so a pH-jump instrument using a nanosecond pulsed laser at 355 nm was built to study the process quantitatively. As shown in Fig. 7, the redissolution kinetics is very fast, reaching equilibrium after less than 10 ms, which is very favorable for the intended use. The curve can be well fitted by a single-exponential function in the form of $I = 0.0075 + 0.92e^{-t/0.85}$ with a characteristic relaxation time $\tau = 0.85$ ms. Note that this fast relaxation process could not be followed by a conventional stopped-flow method because of a dead time of 2–4 ms. Although the redissolution is so fast, from the practical point of view, the pH drop necessary for redissolution (~3 pH units) is too big to take place even in the case of local inflammation or heavy physical exercise. Therefore, this would be probably not a problem for the intended use of our system.

However, disregarding our knowledge of solution behavior and the redissolution process in our depot formulation, the real biological behavior may be obtained only from an in vivo animal experiment. Thus, the polymers were injected i.m. with

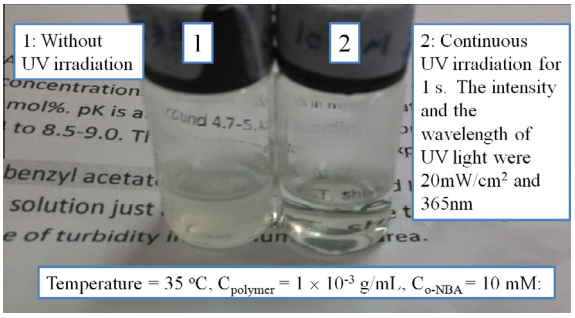

Fig. 6. Redissolution of the phase-separated polymer after acidification by the photoacid *o*-nitrobenzaldehyde and irradiation with a continuous UV source (Hamamatsu, LC8), where the concentrations of the polymer and *o*-nitrobenzaldehyde were 1 mg/mL and 10 mM, respectively. The intensity and the wavelength of the UV light were 20 mW/cm^2 and 365 nm.

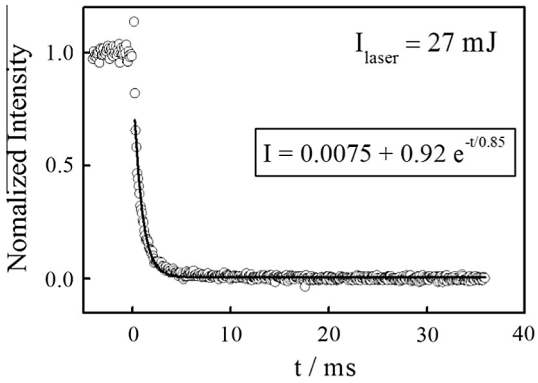

Fig. 7. Time dependence of the normalized scattered light intensities during the redissolution of the phase-separated polymer by a pH jump of ~3 units at 35.0 °C, where the concentrations of the polymer and *o*-nitrobenzaldehyde were 2 mg/mL and 10 mM, respectively. The intensity of the 355 nm pulse laser was 27 mJ.

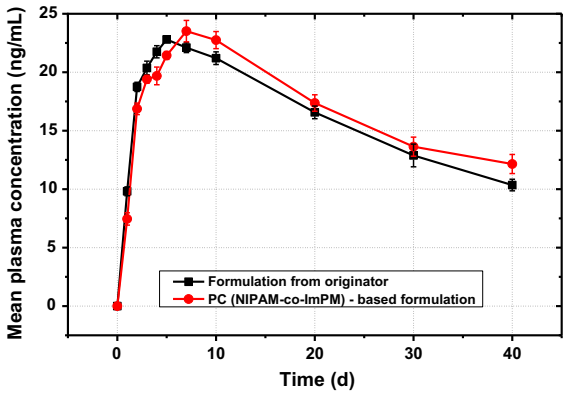

Fig. 8. Plasma concentration of paliperidone palmitate with different formulations.

the model drug paliperidone palmitic acid salt (i.e., the salt, not the prodrug) in a rat animal model, and the ability of the polymer depot to control the sustained release of the active component was compared to the commercial formulation using the enzymatically activated paliperidone palmitic acid ester prodrug, which is known to cause local irritation.

All animals survived the entire study throughout a duration of 6 months without signs of toxicity or local inflammation. During a histopathological evaluation of the injection site, no irritation or cyst formation was observed. No histopathological changes were observed in the organs critical for this active pharmaceutical ingredient (adrenal glands, kidneys, mammary glands, ovaria, spleen and hypophysis). Our PNIPAm-*co*-InPM-based formulation provides excellent control of a prolonged release of paliperidone from the depot (see Fig. 8) with the same release rate as the commercial formulation that causes local irritation. In contrast to the commercial brand, there was also no local irritation observed for our aqueous PNIPAm-*co*-InPM-based formulation. Therefore, the same drug release profile is feasible with the salt of the active drug instead of the enzymatically activated prodrug (with all its drawbacks related to fluctuating local enzymatic activity levels), which brings among others very significant legislative benefits.

4. Conclusions

In this article, we describe a new approach to thermoresponsive polymer-based local depot formulations based on dual pH- and temperature-responsive polymers. Injection is possible in the form of a solution at pH ca. 5 without the risk of injection needle obstruction, and a depot is formed at the application site upon heating to body temperature and the simultaneous pH increase to the physiological value of 7.4. An in vivo experiment with the polymer in PBS (pH = 5.0) and paliperidone as a model drug showed excellent results regarding the release of the drug from the depot.

Acknowledgements

The authors acknowledge financial support from the Ministry of Education, Youth and Sports of the Czech Republic (grant No. KONTAKT LH14292) and the National Natural Scientific Foundation of China (NNSFC) Projects (21274140). S.F.

acknowledges the Czech Science Foundation Grant No. 15-10527J. Dr. Xiaodong Ye thanks Prof. Chi Wu for his valuable comments about the manuscript and Prof. Xiaoguo Zhou for his kind assistance during the experiments. Nikolai Matushkin is acknowledged for his help with the synthesis of PNIPAm-*co*-InPM copolymers. Maria Rabyk is acknowledged for her help with the turbidity measurements.

Appendix A. Supplementary material

Supplementary data associated with this article can be found, in the online version, at http://dx.doi.org/10.1016/j.eurpolymj.2016.09.010.

References

[1] L. Citrome, New second-generation long-acting injectable antipsychotics for the treatment of schizophrenia, Expert Rev Neurother 13 (2013) 767–783, http://dx.doi.org/10.1586/14737175.2013.811984.
[2] M. Graffino, C. Montemagni, C. Mingrone, P. Rocca, Antipsicotici a rilascio prolungato nel trattamento della schizofrenia: una revisione della letteratura, Riv Psichiatr 49 (2014) 115–123.
[3] K. Kühn, K. Wiedemann, R. Hellweg, H. Möller, Stellenwert von Depotformulierungen in der Langzeittherapie der Schizophrenie, Fortschr Der Neurol Psychiatr 82 (2014) 557–565, http://dx.doi.org/10.1055/s-0034-1385108.
[4] P. Llorca, M. Abbar, P. Courtet, S. Guillaume, S. Lancrenon, L. Samalin, Guidelines for the use and management of long-acting injectable antipsychotics in serious mental illness, BMC Psychiatr 13 (2013) 340, http://dx.doi.org/10.1186/1471-244X-13-340.
[5] A.-S. Rauch, W.W. Fleischhacker, Long-acting injectable formulations of new-generation antipsychotics: a review from a clinical perspective, CNS Drugs 27 (2013) 637–652, http://dx.doi.org/10.1007/s40263-013-0083-9.
[6] L. Samalin, A. Nourry, T. Charpeaud, P.-M. Llorca, What is the evidence for the use of second-generation antipsychotic long-acting injectables as maintenance treatment in bipolar disorder?, Nord J Psychiatry 68 (2014) 227–235, http://dxdoi.org/10.3109/08039488.2013.801078.
[7] S. Rahimian, M.F. Fransen, J.W. Kleinovink, J.R. Christensen, M. Amidi, W.E. Hennink, F. Ossendorp, Polymeric nanoparticles for co-delivery of synthetic long peptide antigen and poly IC as therapeutic cancer vaccine formulation, J Control Release 203 (2015) 16–22, http://dx.doi.org/10.1016/j.jconrel.2015.02.006.
[8] R.J. Meyer, M. Mann, Pulmonary oil micro-embolism (POME) syndrome: a review and summary of a large case series, Curr Med Res Opin 31 (2015) 837–841, http://dx.doi.org/10.1185/03007995.2015.1012254.
[9] L. Citrome, Paliperidone palmitate – review of the efficacy, safety and cost of a new second-generation depot antipsychotic medication, Int J Clin Pract 64 (2009) 216–239, http://dx.doi.org/10.1111/j.1742-1241.2009.02240.x.
[10] S. Gentile, Adverse effects associated with second-generation antipsychotic long-acting injection treatment: a comprehensive systematic review, Pharmacother J Hum Pharmacol Drug Ther 33 (2013) 1087–1106, http://dx.doi.org/10.1002/phar.1313.
[11] P. Chue, J. Chue, A review of paliperidone palmitate, Expert Rev Neurother 12 (2012) 1383–1397, http://dx.doi.org/10.1586/ern.12.137.
[12] T.M. Dadhaniya, O.P. Sharma, M.C. Gohel, P.J. Mehta, Current approaches for in vitro drug release study of long acting parenteral formulations, Curr Drug Deliv 12 (2015) 256–270.
[13] F. Pervaiz, M. Ahmad, G. Murtaza, Phase sensitive biodegradable polymer based in situ implant of olanzapine for depot injectable formulation: in vitro release and in vivo absorption in rats, Curr Pharm Anal 11 (2015) 286–291, http://dx.doi.org/10.2174/1573412911666150408223837.
[14] A.L. Silva, R.A. Rosalia, E. Varypataki, S. Sibuea, F. Ossendorp, W. Jiskoot, Poly-(lactic-co-glycolic-acid)-based particulate vaccines: particle uptake by dendritic cells is a key parameter for immune activation, Vaccine 33 (2015) 847–854, http://dx.doi.org/10.1016/j.vaccine.2014.12.059.
[15] R. Vaishya, V. Khurana, S. Patel, A.K. Mitra, Long-term delivery of protein therapeutics, Expert Opin Drug Delivery 12 (2015) 415–440, http://dx.doi.org/10.1517/17425247.2015.961420.
[16] O. Ahmed, K. Hosny, M. Al-Sawahli, U. Fahmy, Optimization of caseinate-coated simvastatin-zein nanoparticles: improved bioavailability and modified release characteristics, Drug Des Devel Ther (2015) 655, http://dx.doi.org/10.2147/DDDT.S76194.
[17] A.H. Hassan, K.M. Hosny, Z.A. Murshid, A. Alhadlaq, A. Alyamani, G. Naguib, Depot injectable biodegradable nanoparticles loaded with recombinant human bone morphogenetic protein-2: preparation, characterization, and in vivo evaluation, Drug Des Devel Ther 9 (2015) 3599–3606, http://dx.doi.org/10.2147/DDDT.S79812.
[18] K.P. Pagar, P. radee, R. Vavia, Naltrexone-loaded poly[La–(Glc–Leu)] polymeric microspheres for the treatment of alcohol dependence: in vitro characterization and in vivo biocompatibility assessment, Pharm Dev Technol 19 (2014) 385–394, http://dx.doi.org/10.3109/10837450.2013.784334.
[19] S. Kim, H. Solari, P.J. Weiden, J.R. Bishop, Paliperidone palmitate injection for the acute and maintenance treatment of schizophrenia in adults, Patient Prefer Adher 6 (2012) 533–545.
[20] A. Alexander, Ajazuddin, J. Khan, S. Saraf, S. Saraf, Poly(ethylene glycol)–poly(lactic-co-glycolic acid) based thermosensitive injectable hydrogels for biomedical applications, J Control Release 172 (2013) 715–729, http://dx.doi.org/10.1016/j.jconrel.2013.10.006.
[21] M. Hruby, P. Pouckova, M. Zadinova, J. Kucka, O. Lebeda, Thermoresponsive polymeric radionuclide delivery system—an injectable brachytherapy, Eur J Pharm Sci 42 (2011) 484–488, http://dx.doi.org/10.1016/j.ejps.2011.02.002.
[22] R. Kamel, M. Basha, S. El Awdan, Development and evaluation of long-acting epidural "smart" thermoreversible injection loaded with spray-dried polymeric nanospheres using experimental design, J Drug Target 21 (2013) 277–290, http://dx.doi.org/10.3109/1061186X.2012.747527.
[23] T. Kojarunchitt, S. Hook, S. Rizwan, T. Rades, S. Baldursdottir, Development and characterisation of modified poloxamer 407 thermoresponsive depot systems containing cubosomes, Int J Pharm 408 (2011) 20–26, http://dx.doi.org/10.1016/j.ijpharm.2011.01.037.
[24] J. Kučka, M. Hrubý, O. Lebeda, Biodistribution of a radiolabelled thermoresponsive polymer in mice, Appl Radiat Isot 68 (2010) 1073–1078, http://dx.doi.org/10.1016/j.apradiso.2010.01.022.
[25] S. Zhang, D.J. Alvarez, M.V. Sofroniew, T.J. Deming, Design and synthesis of nonionic copolypeptide hydrogels with reversible thermoresponsive and tunable physical properties, Biomacromolecules 16 (2015) 1331–1340, http://dx.doi.org/10.1021/acs.biomac.5b00124.
[26] T.R. Hoare, D.S. Kohane, Hydrogels in drug delivery : progress and challenges, Polymer 49 (2008) 1993–2007, http://dx.doi.org/10.1016/j.polymer.2008.01.027.
[27] M.P. Chapman, J.L. Jopez Gonzalez, B.E. Goyette, K.L. Fujimoto, Z. Ma, W.R. Wagner, M.A. Zenati, C.N. Riviere, Application of the HeartLander crawling robot for injection of a thermally sensitive anti-remodeling agent for myocardial infarction therapy, Eng. Med. Biol. Soc. (EMBC), in: 2010 Annu. Int. Conf. IEEE, 2010, pp. 5428–5431. http://dx.doi.org/10.1109/IEMBS.2010.5626518.
[28] T.D. Johnson, K.L. Christman, Injectable hydrogel therapies and their delivery strategies for treating myocardial infarction, Expert Opin Drug Del 10 (2013) 59–72, http://dx.doi.org/10.1517/17425247.2013.739156.
[29] C.T. Huynh, M.K. Nguyen, D.S. Lee, Injectable block copolymer hydrogels: achievements and future challenges for biomedical applications, Macromolecules 44 (2011) 6629–6636, http://dx.doi.org/10.1021/ma201261m.
[30] Y. Maeda, H. Yamamoto, I. Ikeda, Effects of ionization of incorporated imidazole groups on the phase transitions of poly (N-isopropylacrylamide), poly (N,N-diethylacrylamide), and poly (N-vinylcaprolactam) in water, Langmuir 17 (2001) 6855–6859, http://dx.doi.org/10.1021/la0106438.

[31] Y.Y. Khine, Y. Jiang, A. Dag, H. Lu, M.H. Stenzel, Dual-responsive ph and temperature sensitive nanoparticles based on methacrylic acid and di(ethylene glycol) methyl ether methacrylate for the triggered release of drugs, Macromol Biosci 15 (2015) 1091–1104, http://dx.doi.org/10.1002/mabi.201500057.
[32] N.M. Matsumoto, G.W. Buchman, L.H. Rome, H.D. Maynard, Dual pH- and temperature-responsive protein nanoparticles, Eur Polym J 69 (2015) 532–539, http://dx.doi.org/10.1016/j.eurpolymj.2015.01.043.
[33] Q. Zhang, Z. Hou, B. Louage, D. Zhou, N. Vanparijs, B.G. De Geest, R. Hoogenboom, Acid-labile thermoresponsive copolymers that combine fast pH-triggered hydrolysis and high stability under neutral conditions, Angew Chem – Int. Ed. 54 (2015) 10879–10883, http://dx.doi.org/10.1002/anie.201505145.
[34] D. Fournier, R. Hoogenboom, H.M.L. Thijs, R.M. Paulus, U.S. Schubert, D. Fournier, R. Hoogenboom, H.M.L. Thijs, R.M. Paulus, U.S. Schubert, Tunable pH- and Temperature-Sensitive Copolymer Libraries by Reversible Addition − Fragmentation Chain Transfer Copolymerizations of Methacrylates Tunable pH- and Temperature-Sensitive Copolymer Libraries by Reversible Addition – Fragmentation Chain Trans., 2007, pp. 915–920. http://dx.doi.org/10.1021/ma062199r.
[35] J. Jakes, Testing of the constrained regularization method of inverting laplace transform on simulated very wide quasielastic light-scattering aut-correlation functions, Czech J Phys 38 (1988) 1305–1316.
[36] Y. Lu, X. Ye, J. Li, C. Li, S. Liu, Kinetics of laser-heating-induced phase transition of poly(N-isopropylacrylamide) chains in dilute and semidilute solutions, J. Phys. Chem. B 115 (2011) 12001–12006, http://dx.doi.org/10.1021/jp204853p.
[37] X. Ye, Y. Lu, L. Shen, Y. Ding, S. Liu, G. Zhang, C. Wu, How many stages in the coil-to-globule transition of linear homopolymer chains in a dilute solution?, Macromolecules 40 (2007) 4750–4752, http://dxdoi.org/10.1021/ma070167d.
[38] D. Leng, H. Chen, G. Li, M. Guo, Z. Zhu, L. Xu, Y. Wang, Development and comparison of intramuscularly long-acting paliperidone palmitate nanosuspensions with different particle size, Int J Pharm 472 (2014) 380–385, http://dx.doi.org/10.1016/j.ijpharm.2014.05.052.
[39] M. Kissel, P. Peschke, V. Subr, K. Ulbrich, J. Schuhmacher, J. Debus, E. Friedrich, No title synthetic macromolecular drug carriers: biodistribution of poly [(N-2-hydroxypropyl)methacrylamide] copolymers and their accumulation in solid rat tumors, PDA J Pharm Sci Technol 55 (2001) 191–201.
[40] Y.H. Bae, K. Park, Targeted drug delivery to tumors: myths, reality and possibility, J Control Release 153 (2011) 198–205, http://dx.doi.org/10.1016/j.jconrel.2011.06.001.
[41] M.E. Fox, F.C. Szoka, J.M.J. Fréchet, Soluble polymer carriers for the treatment of cancer: the importance of molecular architecture, Acc Chem Res 42 (2009) 1141–1151, http://dx.doi.org/10.1021/ar900035f.
[42] B. Chen, K. Jerger, J.M.J. Fréchet, F.C. Szoka, The influence of polymer topology on pharmacokinetics: differences between cyclic and linear PEGylated poly(acrylic acid) comb polymers, J Control Release 140 (2009) 203–209, http://dx.doi.org/10.1016/j.jconrel.2009.05.021.
[43] C.L. McCormick, A.B. Lowe, Aqueous RAFT polymerization: recent developments in synthesis of functional water-soluble (Co)polymers with controlled structures, Acc Chem Res 37 (2004) 312–325, http://dx.doi.org/10.1021/ar0302484.
[44] H. Schild, D. Tirrell, Microcalorimetric detection of lower critical solution temperatures in aqueous polymer solutions, J Phys Chem 94 (1990) 4352–4356, http://dx.doi.org/10.1021/j100373a088.
[45] S. Furyk, Y. Zhang, D. Ortiz-Acosta, P.S. Cremer, D.E. Bergbreiter, Effects of end group polarity and molecular weight on the lower critical solution temperature of poly(N-isopropylacrylamide), J Polym Sci, Part A: Polym Chem 44 (2006) 1492–1501, http://dx.doi.org/10.1002/pola.21256.
[46] M. Hruby, C. Konak, J. Kucka, M. Vetrik, S.K. Filippov, D. Vetvicka, H. Mackova, G. Karlsson, K. Edwards, B. Rihova, K. Ulbrich, Thermoresponsive, hydrolytically degradable polymer micelles intended for radionuclide delivery, Macromol Biosci 9 (2009) 1016–1027, http://dx.doi.org/10.1002/mabi.200900083.
[47] P.C. Naha, K. Bhattacharya, T. Tenuta, K.a. Dawson, I. Lynch, A. Gracia, F.M. Lyng, H.J. Byrne, Intracellular localisation, geno- and cytotoxic response of polyN-isopropylacrylamide (PNIPAM) nanoparticles to human keratinocyte (HaCaT) and colon cells (SW 480), Toxicol Lett 198 (2010) 134–143, http://dx.doi.org/10.1016/j.toxlet.2010.06.011.
[48] M.A. Cooperstein, H.E. Canavan, Assessment of cytotoxicity of (N-isopropyl acrylamide) and poly(N-isopropyl acrylamide)-coated surfaces, Biointerphases 8 (2013) 19, http://dx.doi.org/10.1186/1559-4106-8-19.
[49] Y.J. Che, Y. Tan, J. Cao, G.Y. Xu, A study of aggregation behavior of a sulfobetaine copolymer in dilute solution, J Polym Res 17 (2010) 557–566, http://dx.doi.org/10.1007/s10965-009-9344-1.
[50] V. Chytry, M. Netopilik, M. Bohdanecky, K. Ulbrich, Phase transition parameters of potential thermosensitive drug release systems based on polymers of N-alkylmethacrylamides, J Biomater Sci Polym Ed 8 (1997) 817–824, http://dx.doi.org/10.1163/156856297X00010.
[51] V. Chytryt, K. Ulbrich, Conjugate of doxorubicin with a thermosensitive polymer drug carrier, J. Bioact. Compat. Polym. Biomed. Appl. 16 (2001) 427–440, http://dx.doi.org/10.1106/FDUM-1LXE-WGJ9-BYVW.
[52] J.D. Ziebarth, Y. Wang, Understanding the protonation behavior of linear polyethylenimine in solutions through Monte Carlo simulations, Biomacromolecules 11 (2010) 29–38, http://dx.doi.org/10.1021/bm900842d.
[53] Y. Maeda, T. Higuchi, I. Ikeda, Change in hydration state during the coil−globule transition of aqueous solutions of poly(N-isopropylacrylamide) as evidenced by FTIR spectroscopy, Langmuir 16 (2000) 7503–7509, http://dx.doi.org/10.1021/la0001575.
[54] M. Hruby, S.K. Filippov, J. Panek, M. Novakova, H. Mackova, J. Kucka, D. Vetvicka, K. Ulbrich, Polyoxazoline thermoresponsive micelles as radionuclide delivery systems, Macromol Biosci 10 (2010) 916–924, http://dx.doi.org/10.1002/mabi.201000034.
[55] X. Wang, X. Qiu, C. Wu, Comparison of the coil-to-globule and the globule-to-coil transitions of a single poly(N -isopropylacrylamide) homopolymer chain in water, Macromolecules 31 (1998) 2972–2976, http://dx.doi.org/10.1021/ma971873p.
[56] S. Hocine, M.-H. Li, Thermoresponsive self-assembled polymer colloids in water, Soft. Matter. 9 (2013) 5839, http://dx.doi.org/10.1039/c3sm50428j.
[57] Y. Zhang, C.Y. Ang, M. Li, S.Y. Tan, Q. Qu, Z. Luo, Y. Zhao, Polymer-coated hollow mesoporous silica nanoparticles for triple-responsive drug delivery, ACS Appl. Mater. Interfaces 7 (2015) 18179–18187, http://dx.doi.org/10.1021/acsami.5b05893.
[58] L. Guo, J. Guan, B. Lin, H. Yang, Synthesis and characterization of methacrylate matrix resin bearing o-nitrobenzyl group, J. Cent. South Univ. 22 (2015) 3296–3301.